Supplementary Material for

SVD-aided non-orthogonal decomposition (SANOD) method to exploit prior knowledge of spectral components in the analysis of time-resolved data

H. Ki[a], Y. Lee[a,b], E. H. Choi[a,b], S. Lee[a,b], and H. Ihee[*a,b]

*E-mail: hyotcherl.ihee@kaist.ac.kr

This PDF file includes:

- **Supplementary Discussions**
- **Supplementary Methods**
- **Supplementary Figures**
- **Supplementary References**

I. Supplementary Discussions

A. Theory of LCF using the direct method

Let us treat a spectrum in experimental time-resolved data as a column vector. This treatment is acceptable because even when the experimental data are obtained in the form of a multidimensional matrix, they can be easily transformed into a column vector using vectorization. For example, in the case of TRXL, the difference scattering curve at a specific time delay, $\Delta S(q, t)$, is expressed as follows:

$$\Delta S(q, t) = [\Delta S(q_1, t), \Delta S(q_2, t), \ldots, \Delta S(q_N, t),]^T \quad \text{(S1)}$$

where T denotes the transpose of a row vector to a column vector. Further, the series of time-resolved data can be approximated as the sum of their time-independent spectral components as follows:

$$\begin{aligned}
\Delta S(q, t_1) &= \Delta S_{sum}(q, t_1) + X(q, t_1) \\
&= \alpha_1(t_1) \cdot C_1(q) + \alpha_2(t_1) \cdot C_2(q) + \cdots + \alpha_n(t_1) \cdot C_n(q) + X(q, t_1) \\
\Delta S(q, t_2) &= \Delta S_{sum}(q, t_2) + X(q, t_2) \\
&= \alpha_1(t_2) \cdot C_1(q) + \alpha_2(t_2) \cdot C_2(q) + \cdots + \alpha_n(t_2) \cdot C_n(q) + X(q, t_2) \\
&\vdots \\
\Delta S(q, t_n) &= \Delta S_{sum}(q, t_n) + X(q, t_n) \\
&= \alpha_1(t_n) \cdot C_1(q) + \alpha_2(t_n) \cdot C_2(q) + \cdots + \alpha_n(t_n) \cdot C_n(q) + X(q, t_n)
\end{aligned} \quad \text{(S2)}$$

where $C_i(q)$ are the spectral components of the signal, $\alpha_i(t_j)$ are their weights at time delay t_j, $\Delta S_{sum}(q, t_j)$ is the approximated signal as the sum of the time-independent spectral components, and $X(q, t_j)$ is a residual signal in $\Delta S(q, t_j)$ for the approximation. When the spectral components, $\{C_i(q)\}_i$, are orthogonal as in the case of singular spectral modes in SVD analysis, the weight of a spectral component, $C_i(q)$, can be easily calculated using vector projection as follows:

$$\alpha_i(t_j) = \frac{< \Delta S(q, t_j), C_i(q) >}{< C_i(q), C_i(q) >} \quad \text{(S3)}$$

where $< A, B >$ denotes the inner product between two vectors, A and B. As shown in Equations (S1)–(S3), direct arithmetical vector projection gives the weight of a component. However, if $\{C_i(q)\}_i$ are not orthogonal, such a simple vector projection does not yield their exact weights in the data.

The non-orthogonal decomposition of SANOD is based on LCF of experimental data

as the sum of the signal components. SANOD uses non-orthogonal signal components as the initial input and obtain their weights. For the latter step, SANOD utilizes the direct method which refers to linear algebraic methods to yield the solution of linear equations without numerical iterative minimization. Among the direct methods, we decided to use QR decomposition to decompose the experimentally observed signal into a sum of the non-orthogonal components, $\{C_i(q)\}_i$.

The entire procedure of SANOD consists of four steps, and it can be briefly described as follows (see Figure S1). The first step is QR decomposition, which is a well-established mathematical procedure for decomposing a matrix into a product of two matrices Q and R, where Q is an orthogonal matrix and R is an upper triangular matrix. A matrix is prepared by horizontally concatenating a set of non-orthogonal components, $\{C_i(q)\}_i$. Then, the matrix is decomposed to yield the Q and R matrices. There are several numerical methods for QR decomposition, such as the Gram-Schmidt (GS) process[1-5], Householder reflections[6-10], and Givens rotations[10,11], each of which has its own advantages and disadvantages. In this study, the GS process, which is a textbook example of a method for orthonormalization of a set of vectors, is implemented for the QR decomposition, because it is easy to visualize and express using mathematical formula. The GS orthonormalization of a set of non-orthogonal signal components, $\{C_i(q)\}_i$, yields a set of orthonormalized signal components, $\{O_i(q)\}_i$ (see Figure S1b). The process can be formulated as follows:

$$
\begin{aligned}
O_1 &= norm\left(\frac{C_1}{|C_1|}\right) = \frac{C_1}{\beta_{1,1}} \\
O_2 &= norm(C_2 - proj(C_2, O_1)) \\
&= \frac{(C_2 - \beta_{1,2} \cdot O_1)}{\beta_{2,2}} \\
O_3 &= norm(C_3 - proj(C_3, O_1) - proj(C_3, O_2)) \\
&= \frac{(C_3 - \beta_{1,3} \cdot O_1 - \beta_{2,3} \cdot O_2)}{\beta_{3,3}} \\
&\vdots \\
O_n &= norm(C_n - proj(C_n, O_1) - proj(C_n, O_2) - \cdots
\end{aligned}
\tag{S4}
$$

$$- proj(C_n, O_{n\text{-}1}))$$
$$= \frac{(C_n - \beta_{1,n} \cdot O_1 - \beta_{2,n} \cdot O_2 - \cdots - \beta_{n\text{-}1,n} \cdot O_{n\text{-}1})}{\beta_{n,n}}$$

while $\beta_{i,j}$ are constants, $norm(A)$ denotes the normalized vector of A, which can be expressed as $A \ / \sqrt{< A, A >}$, $|A|$ denotes the magnitude of vector A, and $proj(A, B)$ stands for the projection of vector A to vector B, which can be expressed as

$$\frac{< A, B >}{< B, B >} \cdot B \tag{S5}$$

Note that $\beta_{i,j} = < C_j(q), O_i(q) >$. It is obvious that the resulting $\{O_i(q)\}_i$ are orthogonal. Horizontal concatenation of $\{O_i(q)\}_i$ yields the matrix Q, and the matrix with the element $\beta_{i,j}$ in its ith row and jth column is the matrix R.

The second step is to calculate the weight of a signal component, $C_n(q)$, by using the orthogonalized components (see Figure S1c). From Equation (S4), $\{C_i(q)\}_i$ can be expressed in terms of $\{O_i(q)\}_i$ as

$$\begin{aligned} C_1 &= \beta_{1,1} \cdot O_1 \\ C_2 &= \beta_{1,2} \cdot O_1 + \beta_{2,2} \cdot O_2 \\ C_3 &= \beta_{1,3} \cdot O_1 + \beta_{2,3} \cdot O_2 + \beta_{3,3} \cdot O_3 \\ &\vdots \\ C_n &= \beta_{1,n} \cdot O_1 + \beta_{2,n} \cdot O_2 + \cdots + \beta_{n,n} \cdot O_n \end{aligned} \tag{S6}$$

Substituting Equation (S6) into Equation (S2) yields

$$\begin{aligned} \Delta S(q, t_j) &= \Delta S_{sum}(q, t_j) + X(q, t_j) \\ &= \alpha_1(t_j) * C_1(q) + \alpha_2(t_j) * C_2(q) + \cdots + \alpha_n(t_j) * C_n(q) + X(q, t_j) \\ &= \beta_{1,1} \cdot \alpha_1(t_j) \cdot O_1(q) + \alpha_2(t_j) \cdot (\beta_{1,2} \cdot O_1(q) + \beta_{2,2} \cdot O_2(q)) + \cdots \\ &\quad + \alpha_n(t_j) \cdot (\beta_{1,n} \cdot O_1(q) + \beta_{2,n} \cdot O_2(q) + \cdots + \beta_{n\text{-}1,n} \cdot O_{n\text{-}1}(q) \\ &\qquad + \beta_{n,n} \cdot O_n(q)) + X(q, t_j) \end{aligned} \tag{S7}$$

In Equation (S7), the only constant in the term of $O_n(q)$ is $\beta_{n,n} \cdot \alpha_n(t_j)$. Therefore, by taking the inner product with $O_n(q)$ on both sides of Equation (S7), $\alpha_n(t_j)$ can be arithmetically calculated as

$$< \Delta S(q, t_j), O_n(q) > = \beta_{n,n} \cdot \alpha_n(t_j) \cdot < O_n(q), O_n(q) > \tag{S8}$$

$$= \beta_{n,n} \cdot \alpha_n(t_j)$$

$$\alpha_n(t_j) = \frac{< \Delta S(q, t_j), O_n(q) >}{\beta_{n,n}}$$

The first step, QR decomposition, is essential for the second step because the weights of the non-orthogonalized signal components, $\alpha_n(t_j)$, can be simply calculated on the basis of the orthogonal properties of $\{O_i(q)\}_i$.

The third step is to remove the contribution of the $C_n(q)$ component from the signal (see Figure S1d). By using the weight $\alpha_n(t_j)$ calculated in the second step, the known contribution of the component $C_n(q)$ can be subtracted from the signal as follows:

$$\begin{aligned} &\Delta S(q, t_j) - \alpha_n(t_j) \cdot C_n(q) \\ &= \alpha_1(t_j) \cdot C_1(q) + \alpha_2(t_j) \cdot C_2(q) + \cdots + \alpha_{n-1}(t_j) \cdot C_{n-1}(q) + X(q, t_j) \\ &= \alpha_1(t_j) \cdot \beta_{1,1} \cdot O_1(q) + \alpha_2(t_j) \cdot (\beta_{1,2} \cdot O_1(q) + \beta_{2,2} \cdot O_2(q)) + \cdots \\ &+ \alpha_{n-1}(t_j) \cdot (\beta_{1,n-1} \cdot O_1(q) + \cdots + \beta_{n-1,n-1} \cdot O_{n-1}(q)) + X(q, t_j) \end{aligned} \quad \text{(S9)}$$

The fourth step is to simply repeat the second and third steps until the weights of all the components are calculated. As the contribution of the nth component, $C_n(q)$, is subtracted from the signal, the remaining signal, $\Delta S(q, t_j) - \alpha_n(t_j) \cdot C_n(q)$, consists of n–1 components from $C_1(q)$ to $C_{n-1}(q)$. By applying the second step to the remaining signal, the weight, $\alpha_{n-1}(t_j)$, of a signal component, $C_{n-1}(q)$, can be calculated as follows.

$$\begin{aligned} &< \Delta S(q, t_j) - \alpha_n(t_j) \cdot C_n(q), O_{n-1}(q) > \\ &= \beta_{n-1,n-1} \cdot \alpha_{n-1}(t_j) \cdot < O_{n-1}(q), O_{n-1}(q) > \\ &= \beta_{n-1,n-1} \cdot \alpha_{n-1}(t_j) \end{aligned} \quad \text{(S10)}$$

$$\alpha_{n-1}(t_j) = \frac{< \Delta S(q, t_j) - \alpha_n(t_j) \cdot C_n(q), O_{n-1}(q) >}{\beta_{n-1,n-1}}$$

Repeating the third step to remove the contribution of the (n–1)th component yields the remaining signal, which consists of n–2 components. By repeating these processes until the last weight, $\alpha_1(t_j)$, is obtained, the set of the weights, $\{\alpha_i(t_j)\}_i$, for all the components at a certain time delay, t_j, is completed. Again, by repeating the procedure for the entire time series of the experimental data, the time-dependent profile of the contribution of each component, $\{\{\alpha_i(t_j)\}_i\}_j$, is obtained. These profiles, which are called chronograms, show when and which processes occur as the reaction progresses. As shown by Equations (S1), (S2), and (S4)–(S10),

the entire procedure to retrieve $\{\{\alpha_i(t_j)\}_i\}_j$ is a fully arithmetic procedure, i.e., no iterative fitting is required. Accordingly, the procedure is not only simple and fast but also yields a unique optimal solution.

Note that the chronogram $\{\{\alpha_i(t_j)\}_i\}_j$ obtained from SANOD is the solution that minimizes the norm of each $X(q, t_j)$ in Equation (S2). In other words, the method finds $\{\{\alpha_i(t_j)\}_i\}_j$ that minimizes the magnitude of the residual signals; thus, the solution obtained from SANOD is the same as that obtained from least-squares fitting.[1] Moreover, it is possible to modify the SANOD procedure to obtain $\{\{\alpha_i(t_j)\}_i\}_j$ that minimizes the weighted least square, such as the chi-square, which exploits the experimental standard deviations. The modification and related discussion are presented in the following section. In the demonstrations presented in the main text, we use the modified SANOD, which minimizes the chi-square of the residual signal.

B. Relationship between SANOD, least-squares minimization, and chi-squared minimization

Part 1. Relationship between SANOD and least-squares minimization

As mentioned in the main text, $\{\alpha_i(t_j)\}_i$, the weights of the components at a certain time delay, t_j, obtained using SANOD are identical to the solution of least-squares fitting of the following equation:

$$\begin{aligned}\Delta S(q, t_j) &= \Delta S_{sum}(q, t_j) + X(q, t_j) \\ &= \alpha_1(t_j) \cdot C_1(q) + \alpha_2(t_j) \cdot C_2(q) + \cdots + \alpha_n(t_j) \cdot C_n(q) + X(q, t_j)\end{aligned} \tag{S11}$$

This can be proved as follows. The orthonormalized components of $\{C_i(q)\}_i$ are denoted as $\{O_i(q)\}_i$. Then, as shown in Equation (S7) in the main text, Equation (S11) can be expressed in terms of $\{O_i(q)\}_i$ as follows:

$$\begin{aligned}\Delta S(q, t_j) &= \Delta S_{sum}(q, t_j) + X(q, t_j) \\ &= \alpha_1(t_j) \cdot C_1(q) + \alpha_2(t_j) \cdot C_2(q) + \cdots + \alpha_n(t_j) \cdot C_n(q) + X(q, t_j) \\ &= \beta_{1,1} \cdot \alpha_1(t_j) \cdot O_1(q) + \alpha_2(t_j) \cdot (\beta_{1,2} \cdot O_1(q) + \beta_{2,2} \cdot O_2(q)) + \cdots \\ &\quad + \alpha_n(t_j) \cdot (\beta_{1,n} \cdot O_1(q) + \cdots + \beta_{n,n} \cdot O_n(q)) + X(q, t_j)\end{aligned} \tag{S12}$$

The residual $X(q, t_j)$ can also be expressed as a sum of $\{O_i(q)\}_i$ components and the residual component, $Z(q, t_j)$,which is orthogonal to all the $O_i(q)$s as follows.

$$X(q, t_j) = \gamma_1(t_j) \cdot O_1(q) + \gamma_2(t_j) \cdot O_2(q) + \cdots + \gamma_n(t_j) \cdot O_n(q) + Z(q, t_j) \quad \text{(S13)}$$

Substitution of Equation (S13) into Equation (S12) yields the following equation:

$$\begin{aligned} \Delta S(q, t_j) = {} & O_1(q) \cdot (\beta_{1,1} \cdot \alpha_1(t_j) + \cdots + \beta_{1,n} \cdot \alpha_n(t_j) + \gamma_1(t_j)) + \cdots \\ & + O_n(q) \cdot (\beta_{n,n} \cdot \alpha_n(t_j) + \gamma_n(t_j)) + Z(q, t_j) \end{aligned} \quad \text{(S14)}$$

As mentioned in Equation (S8), $\alpha_n(t_j)$ is obtained as follows:

$$\alpha_n(t_j) = \frac{< \Delta S(q, t_j), O_n(q) >}{\beta_{n,n}} \quad \text{(S15)}$$

Substitution of Equation (S14) into Equation (S15) yields the following equation because $O_n(q)$ is orthogonal to the other $O_i(q)$s and $Z(q, t_j)$:

$$\begin{aligned} \alpha_n(t_j) &= \frac{< \Delta S(q, t_j), O_n(q) >}{\beta_{n,n}} \\ &= \frac{\beta_{n,n} \cdot \alpha_n(t_j) + \gamma_n(t_j)}{\beta_{n,n}} \\ &= \alpha_n(t_j) + \frac{\gamma_n(t_j)}{\beta_{n,n}} \end{aligned} \quad \text{(S16)}$$

Equation (S16) indicates that $\gamma_n(t_j)$ must be zero. Thus, it can be shown that $\gamma_i(t_j)$s are zero for all i. Considering Equation (S13), this means that $X(q, t_j)$ is $Z(q, t_j)$ and thereby orthogonal to all the $O_i(q)$s. In summary, SANOD yields the residual component, $X(q, t_j)$, which is orthogonal to all the $O_i(q)$s.

Now, let us consider what is $X(q, t_j)$ obtained from least-squares fitting. According to its definition, least-squares fitting finds $\{\alpha_i(t_j)\}_i$ that minimizes the square of the norm of $X(q, t_j)$. Again, using Equation (S13), $X(q, t_j)$ can be expressed as the sum of $\{O_i(q)\}_i$ components and the residual. Following Equation (S13), the square of the norm of $X(q, t_j)$ can be expressed as follows:

$$\left|X(q, t_j)\right|^2 = {\gamma_1}^2(t_j) + {\gamma_2}^2(t_j) + \cdots + {\gamma_n}^2(t_j) + \left|Z(q, t_j)\right|^2 \quad \text{(S17)}$$

According to Equation (S17), $\left|X(q, t_j)\right|^2$ is minimized when $\gamma_i(t_j)$s are zero for all i. This means that the least-squares fitting yields $\{\alpha_i(t_j)\}_i$ that makes $\gamma_i(t_j)$s zero for all i, i.e., $X(q, t_j)$ equal to $Z(q, t_j)$ and consequently orthogonal to all the $O_i(q)$s. Previously, we showed that SANOD also yields the residual $X(q, t_j)$, which is orthogonal to the $O_i(q)$s. Thus, so far we

have proven that both SANOD and least-squares fitting yield $X(q, t_j)$, which is orthogonal to the $O_i(q)$s. Such a residual component is uniquely defined as follows:

$$X(q, t_j) = \Delta S(q, t_j) - \sum_i proj(\Delta S(q, t_j), O_i) \quad \text{(S18)}$$

The uniqueness of $X(q, t_j)$ ensures that the residual from SANOD is identical to the residual from the least-squares fitting. As the residuals are the same for SANOD and the least-squares fitting, $\Delta S_{sum}(q, t_j)$s also should be the same for the two methods. When $\Delta S_{sum}(q, t_j)$ is determined, $\alpha_i(t_j)$ s are uniquely derived from $\Delta S_{sum}(q, t_j)$ if $\{C_i(q)\}_i$ are linearly independent. Suppose that $\{C_i(q)\}_i$ are linearly independent and there are two different solutions of $\alpha_i(t_j)$s, $\alpha_i'(t_j)$s and $\alpha_i''(t_j)$s, yielding the same $\Delta S_{sum}(q, t_j)$. Then, the following equations hold.

$$\Delta S_{sum}(q, t_j) = \sum_i \alpha_i'(t_j) \cdot C_i(q) \quad \text{(S19)}$$

$$\Delta S_{sum}(q, t_j) = \sum_i \alpha_i''(t_j) \cdot C_i(q) \quad \text{(S20)}$$

As $\alpha_i'(t_j)$s and $\alpha_i''(t_j)$s are different, there exists an index d that satisfies $\alpha_d'(t_j) \neq \alpha_d''(t_j)$. Substitution of Equation (S20) into Equation (S19) yields the following equations:

$$\sum_i \alpha_i'(t_j) \cdot C_i(q) = \sum_i \alpha_i''(t_j) \cdot C_i(q) \quad \text{(S21)}$$

$$\sum_i \{(\alpha_i'(t_j) - \alpha_i''(t_j)) \cdot C_i(q)\} = 0 \quad \text{(S22)}$$

$$\sum_{i \neq d} \{(\alpha_i'(t_j) - \alpha_i''(t_j)) \cdot C_i(q)\} = (\alpha_d''(t_j) - \alpha_d'(t_j)) \cdot C_d(q) \quad \text{(S23)}$$

Equation (S23) contradicts the assumption that $\{C_i(q)\}_i$ are linearly independent. The contradiction means that once $\Delta S_{sum}(q, t_j)$ is determined and $\{C_i(q)\}_i$ are linearly independent, then $\{\alpha_i(t_j)\}_i$ must be uniquely determined. As $\Delta S_{sum}(q, t_j)$ from SANOD is identical to $\Delta S_{sum}(q, t_j)$ from the least-squares fitting, finally, it can be concluded that $\{\alpha_i(t_j)\}_i$ obtained using SANOD is identical to that obtained using the least-squares fitting when $\{C_i(q)\}_i$ are linearly independent.

Part 2. Modification of SANOD to yield the solution of chi-squared minimization

When analyzing experimental data, chi-square fitting, which implements the information of standard deviations associated with each data point, is normally preferred over least-squares fitting. Accordingly, it would be highly desirable if SANOD can be modified to obtain the same solution as that of chi-square fitting.

The modification is as follows. The key idea of the modification is to scale the signal components and the experimental data using the standard deviations, and to apply SANOD to the scaled data using the scaled components. This can be done by orthonormalization of the scaled components, $\{C_i(q)/\sigma(q, t_j)\}_i$, to yield $\{O'_i(q, t_j)\}_i$. Then, according to Equation (S17), the scaled experimental data can be expressed in terms of $\{O'_i(q, t_j)\}_i$ as follows:

$$\begin{aligned}\frac{\Delta S(q, t_j)}{\sigma(q, t_j)} &= \frac{\Delta S_{sum}(q, t_j)}{\sigma(q, t_j)} + \frac{X(q, t_j)}{\sigma(q, t_j)} \\ &= \alpha'_1(t_j) \cdot \frac{C_1(q)}{\sigma(q, t_j)} + \alpha'_2(t_j) \cdot \frac{C_2(q)}{\sigma(q, t_j)} + \cdots + \alpha'_n(t_j) \cdot \frac{C_n(q)}{\sigma(q, t_j)} + \frac{X(q, t_j)}{\sigma(q, t_j)} \\ &= \alpha'_1(t_j) \cdot \beta'_{1,1} \cdot O'_1(q, t_j) + \alpha'_2(t_j) \cdot (\beta'_{1,2} \cdot O'_1(q, t_j) \\ &\quad + \beta'_{2,2} \cdot O'_2(q, t_j)) + \cdots + \alpha'_n(t_j) \cdot (\beta'_{1,n} \cdot O'_1(q, t_j) + \cdots \\ &\quad + \beta'_{n,n} \cdot O'_n(q, t_j)) + \frac{X'(q, t_j)}{\sigma(q, t_j)}\end{aligned} \tag{S24}$$

For Equation (S18), α_is, $\beta_{i,j}$s, and $O_i(q, t_j)$s in Equation (S7) are substituted by α'_is, $\beta'_{i,j}$s, and $O'_i(q, t_j)$s to emphasize that the constants and the orthonormalized components obtained from SANOD are different from those obtained from the modified SANOD. Clearly, the resulting equation in terms of $\{O_i(q, t_j)\}_i$ is identical to Equation (S12), except that the residual term $X(q, t_j)$ is substituted by a scaled residual, $X'(q, t_j)/\sigma(q, t_j)$. Therefore, by recalling the discussion in Part 1, it can be deduced that SANOD on the scaled experimental data using scaled signal components will yield $\{\alpha'_i(t_j)\}_i$ that minimizes the square of the norm of $X'(q, t_j)/\sigma(q, t_j)$. Because the square of the norm of $X'(q, t_j)/\sigma(q, t_j)$, $|X'(q, t_j)/\sigma(q, t_j)|^2$, is identical to the chi-square by its definition, the modified SANOD minimizes the chi-square. Accordingly, the modified SANOD yields the same result as the chi-square fitting. Note that the orthonormalized scaled signal components, $\{O'_i(q, t_j)\}_i$, are dependent on the time delay unlike the case of normal SANOD. Clearly, the standard deviation, $\sigma(q, t_j)$, is dependent on

the time delay. Consequently, the scaled signal components, $\{C_i(q)/\sigma(q, t_j)\}_i$, and their orthonormalized ones, $\{O'_i(q, t_j)\}_i$, become dependent on the time delay.

C. Discussion regarding the example of the application of SANOD in the section C-1 of the main text:

The method to retrieve the correct shape of the third component

Normally, the LSVs obtained from SVD do not directly represent physically meaningful spectral component. Instead, a physically meaningful spectral component, e.g. a species-associated spectrum, is represented as a linear combination of the LSVs. As SANOD also uses the LSVs as the spectral components for LCF, to retrieve the correct shape of the physically meaningful spectrum and their kinetics, it is required to perform posterior analysis after SANOD. The detailed procedure is as follows.

The first, and the most important step is to build a correct kinetic model basing on the prior knowledges. In the example in the section C-1, among the three components used for SANOD, the first two components are for the systematic noise of the experiment and are prepared by using prior knowledge on the data. Basing on the prior knowledge, it can be reasonably modeled without any difficulty that the final chronograms of the two components from the posterior analysis should not show any time-dependent trend but noise. In other words, the kinetic model for the two components can be constrained as follows.

$$\alpha_1'(t_j) = \alpha_2'(t_j) = 0 \tag{S25}$$

Primes are attached to the notations of the chronograms in order to distinguish the chronograms for the kinetic model from those obtained from SANOD. The kinetic model for $\alpha'_3(t_j)$ is constrained to follow that from SANOD as follows.

$$\alpha_3'(t_j) = \alpha_3(t_j) \tag{S26}$$

Let the correct shape of the third component, C_3, is C_3'. As C_3' should be represented as a linear combination of C_1, C_2, and C_3, it can be represented as follows,

$$C_3'(q) = \delta \cdot C_1(q) + \varepsilon \cdot C_2(q) + \zeta \cdot C_3(q) \tag{S27}$$

where δ, ε and ζ are the weights for the linear combination. Substituting Equations (S25)-(S27) to Equation (S11) yields

$$\begin{aligned} \Delta S(q, t_j) &= \Delta S_{sum}(q, t_j) + X(q, t_j) \\ &= \alpha_1(t_j) \cdot C_1(q) + \alpha_2(t_j) \cdot C_2(q) + \alpha_3(t_j) \cdot C_3(q) + X(q, t_j) \\ &= \alpha_1'(t_j) \cdot C_1'(q) + \alpha_2'(t_j) \cdot C_2'(q) + \alpha_3'(t_j) \cdot C_3'(q) + X(q, t_j) \end{aligned} \tag{S28}$$

$$= \alpha_3(t_j) \cdot (\delta \cdot C_1(q) + \varepsilon \cdot C_2(q) + \zeta \cdot C_3(q)) + X(q, t_j)$$

Comparison of the second and the fourth rows in Equation (S28) yields,

$$\begin{aligned} &\alpha_1(t_j) \cdot C_1(q) + \alpha_2(t_j) \cdot C_2(q) + \alpha_3(t_j) \cdot C_3(q) \\ &\quad = \alpha_3(t_j) \cdot (\delta \cdot C_1(q) + \varepsilon \cdot C_2(q) + \zeta \cdot C_3(q)) \end{aligned} \tag{S29}$$

Equation (S29) can be solved by finding the set of δ, ε and ζ that fits the following equation.

$$\begin{aligned} &(\delta \cdot \alpha_3(t_j) - \alpha_1(t_j)) \cdot C_1(q) + (\varepsilon \cdot \alpha_3(t_j) - \alpha_2(t_j)) \cdot C_2(q) \\ &\quad + (\zeta \cdot \alpha_3(t_j) - \alpha_3(t_j)) \cdot C_3(q) = 0 \end{aligned} \tag{S30}$$

Since Equation (S30) is linear, the solution of δ, ε and ζ can be solved by using the direct method.

Proof that regardless of whether $U_1(q)$ or $(\partial S(q)/\partial T)_\rho$ is used as the third component in SANOD, the resulting $\alpha_3(t)$ is the same

First, let us consider the case when C_3 is $(\partial S(q)/\partial T)_\rho$. Because $(\partial S(q)/\partial T)_\rho$ of water is a linear combination of C_1, C_2, and U_1, it can be expressed as follows:

$$\left(\frac{\partial S(q)}{\partial T}\right)_\rho = \mu \cdot C_1 + \theta \cdot C_2 + \eta \cdot U_1 \tag{S31}$$

where μ, θ, and η are the weights for the linear combination. Recalling Equation (S4), when C_3 is $(\partial S(q)/\partial T)_\rho$, orthonormalization of the three components yields $\{O_i\}_i$ as follows.

$$\begin{aligned} O_1 &= \frac{C_1}{\beta_{1,1}} \\ O_2 &= \frac{(C_2 - \beta_{1,2} \cdot O_1)}{\beta_{2,2}} \\ O_3 &= \frac{(C_3 - \beta_{1,3} \cdot O_1 - \beta_{2,3} \cdot O_2)}{\beta_{3,3}} \\ &= \frac{(\mu \cdot C_1 + \theta \cdot C_2 + \eta \cdot U_1 - \beta_{1,3} \cdot O_1 - \beta_{2,3} \cdot O_2)}{\beta_{3,3}} \end{aligned} \tag{S32}$$

Since $\beta_{i,j} = < C_j, O_i >$, $\beta_{1,3}$ and $\beta_{2,3}$ are expressed as follows:

$$\begin{aligned} \beta_{1,3} &= < C_3, O_1 > = < \mu \cdot C_1 + \theta \cdot C_2 + \eta \cdot U_1, O_2 > \\ &= \mu \cdot < C_1, O_2 > + \theta \cdot < C_2, O_2 > + \eta \cdot < U_1, O_2 > \\ &= \mu \cdot \beta_{1,1} \cdot < O_1, O_2 > + \theta \cdot < C_2, O_2 > + \eta \cdot < U_1, O_2 > \end{aligned} \tag{S33}$$

Substitution of Equation (S33) and Equation (S6) into Equation (S32) yields the following equation:

$$\begin{aligned} O_3 &= \frac{(\mu \cdot C_1 + \theta \cdot C_2 + \eta \cdot U_1 - \beta_{1,3} \cdot O_1 - \beta_{2,3} \cdot O_2)}{\beta_{3,3}} \\ &= \frac{1}{\beta_{3,3}} \cdot ((\mu \cdot \beta_{1,1} \cdot O_1 + \theta \cdot (\beta_{1,2} \cdot O_1 + \beta_{2,2} \cdot O_2) + \eta \cdot U_1 \\ &\quad - (\mu \cdot \beta_{1,1} + \theta \cdot \beta_{1,2} + \eta \cdot < U_1, O_1 >) \cdot O_1 \\ &\quad - (\theta \cdot \beta_{2,2} + \eta \cdot < U_1, O_2 >) \cdot O_2) \\ &= \frac{(U_1 - < U_1, O_1 > \cdot O_1 - < U_1, O_2 > \cdot O_2) \cdot \eta}{\beta_{3,3}} \end{aligned} \tag{S34}$$

For comparison, let us consider the other case when C_3 is U_1, not $(\partial S(q)/\partial T)_\rho$. Let the

orthonormalization of C_1, C_2, and U_1 yield $\{O_i'\}_i$. In this case, the orthonormalized components can be expressed as follows:

$$
\begin{aligned}
O_1' &= \frac{C_1}{\beta_{1,1}'} = O_1 \\
O_2' &= \frac{C_2 - \beta_{1,2}' \cdot O_1'}{\beta_{2,2}'} = O_2 \\
O_3' &= \frac{U_1 - \beta_{1,3}' \cdot O_1' - \beta_{2,3}' \cdot O_2'}{\beta_{3,3}'} \\
&= \frac{U_1 - \langle U_1, O_1 \rangle \cdot O_1 - \langle U_1, O_2 \rangle \cdot O_2}{\beta_{3,3}'} \\
&= \frac{O_3 \cdot \beta_{3,3}}{\eta \cdot \beta_{3,3}'} = O_3 \cdot \omega
\end{aligned}
\tag{S35}
$$

where ω is a constant. Equation (S35) shows that the two vectors $O_3 \cdot \omega$ and O_3' have the same direction and the same magnitude. Because O_3 and O_3' are both unit vectors, it can be deduced that $\omega = 1$ and O_3 is identical to O_3'. This proves that as $(\partial S(q)/\partial T)_\rho$ of water is a linear combination of C_1, C_2, and $U_1(q)$, the GS process of C_3 yields the same O_3 regardless of whether C_3 is $U_1(q)$ or $(\partial S(q)/\partial T)_\rho$ of water. Therefore, according to Equation (S8), $\alpha_3(t)$ for $U_1(q)$ and $\alpha_3(t)$ for $(\partial S(q)/\partial T)_\rho$ of water are identical.

D. The method to retrieve the correct shape of the signal component from erroneous prior knowledge

When applying prior knowledge on the shape of the signal components to analyze experimental data, there is always a possibility that the prior knowledge contains some errors. Normally, such errors in the shape of the signal components can significantly affect the result of kinetic analysis. For example, the contribution of a signal component can be miscalculated if there are errors in the shape of the signal component. This is also true for the case of SANOD. To demonstrate how the result of SANOD is affected, the experimental data shown in Figure 4a was analyzed using SANOD with an erroneous $(\partial S(q)/\partial T)_\rho$ component. Three components, the two signal components corresponding to the systematic artifacts of the experiment (C_1 and C_2) and an erroneous $(\partial S(q)/\partial T)_\rho$ component, were used for SANOD. The erroneous $(\partial S(q)/\partial T)_\rho$ component was prepared by shifting the q-axis, i.e., by multiplying a constant factor (q-shift) on the q values, of the known correct shape of the signal. A range of factors from 0.99 to 0.94 were tested. Figure S2a shows the generated curves in comparison with the original, correct $(\partial S(q)/\partial T)_\rho$ curve. Figure S2c shows $\alpha_3(t)$ traces for various q-shift factors. As the amount of the error increases, $\alpha_3(t)$ deviates more from $\alpha_3(t)$ obtained from the correct $(\partial S(q)/\partial T)_\rho$ or $U_1(q)$, and accordingly the residual increases as shown in Figure S2d. Also it can be shown that the contribution of the erroneous signal component decreases as the more error is introduced to the shape of the component. Figure S2e shows the residual when the erroneous $(\partial S(q)/\partial T)_\rho$ curve with the q-shift of 0.95 is used. The residual is not negligible anymore. From the residual, $X(q, t)$, we can extract the component, $R(q)$, that has the $\alpha_3(t)$ trace by using the following equation.

$$R(q) = \sum_i (X(q, t_i) \cdot \alpha_3(t_i)) / \sum_i (\alpha_3{}^2(t_i)) \tag{S36}$$

The uppermost curve in Figure S2f is $R(q)$.

Then by using the posterior analysis described in the Section C of the supplementary material, which is the method to retrieve the correct shape of the third component, the wrong weights of the artifacts are corrected to yield the artifact-corrected signal component, that is $C_3'(q)$ in Equation (S27). After that, by adding $R(q)$ to $C_3'(q)$, the final reconstructed signal component is retrieved. As shown in Figure S2g, the reconstructed $(\partial S(q)/\partial T)_\rho$ curve is essentially identical to the correct $(\partial S(q)/\partial T)_\rho$ curve, indicating that the correct $(\partial S(q)/\partial T)_\rho$

can be still obtained by using even the inaccurate, erroneous prior knowledge on the shape of the signal component. Nevertheless it is more convenient to use $U_1(q)$ instead of the known $(\partial S(q)/\partial T)_\rho$ to retrieve the correct $(\partial S(q)/\partial T)_\rho$ because a smaller number of steps are involved.

II. Supplementary Methods

A. TRXL data of CHI_3 in cyclohexane

The TRXL data on CHI_3 in cyclohexane were collected at the ID09B beamline in the European Synchrotron Radiation Facility (ESRF). Details on the experimental scheme and data are described in the previous publication, which reported the structural dynamics based on global analysis.[12]

B. TRXL data of $Au(CN)_2^-$ trimers in water

The TRXL data on $Au(CN)_2^-$ trimers in water were collected at the NW14A beamline in the High Energy Accelerator Research Organization (KEK). Details on the experimental scheme and data are described in the previous publication, which reported the structural dynamics of this molecular system.[13,14]

C. TRXL experiment of a dye molecule in water

The TRXL experiment was performed at the BL3 beamline of SPring-8 Angstrom Compact Free-Electron Laser (SACLA). A typical setup for TRXL was used in the experiment. A femtosecond laser pulse from a Ti:sapphire laser was frequency-doubled to 400 nm and used to initiate the reaction. The laser pulse was focused to a spot of 300 × 200 um^2 to give 3 mJ/mm^2 fluence on the sample. Subsequently, a femtosecond X-ray pulse generated at SACLA was used to probe the progress of the reaction. The X-ray pulse had a center energy of 14.76 keV and was focused to a spot of 20 × 20 um^2 on the sample. The two-dimensional scattering pattern of the X-ray pulse was collected on an area detector (Rayonix LX255-HS) with a sample-to-detector distance of 24.3 mm. For the sample, an aqueous solution of a dye molecule, 4-amino-1,1′-azobenzene-3,4′-disulfonic acid monosodium salt, and sodium hydroxide, with concentrations of 2 mM and 4 mM, respectively, was used. The sample solution was circulated through a sapphire slit nozzle (0.3 mm slit, Kyburz) to form a flat liquid jet. The scattering signal from the solution was measured at the following time delays: from –5 ps to 15 ps in 1 ps steps, 17 ps, 20 ps, 25 ps, 30 ps, 35 ps, 40 ps, 50 ps, 60 ps, 80 ps, and 100 ps. In addition, the signal at a negative time delay, –20 ps, was measured as a reference signal for unexcited ground-state samples. The reference signal was subtracted from the signal from the other time delays to obtain the difference scattering signals, $\Delta S(q, t)$.

III. Supplementary Figures

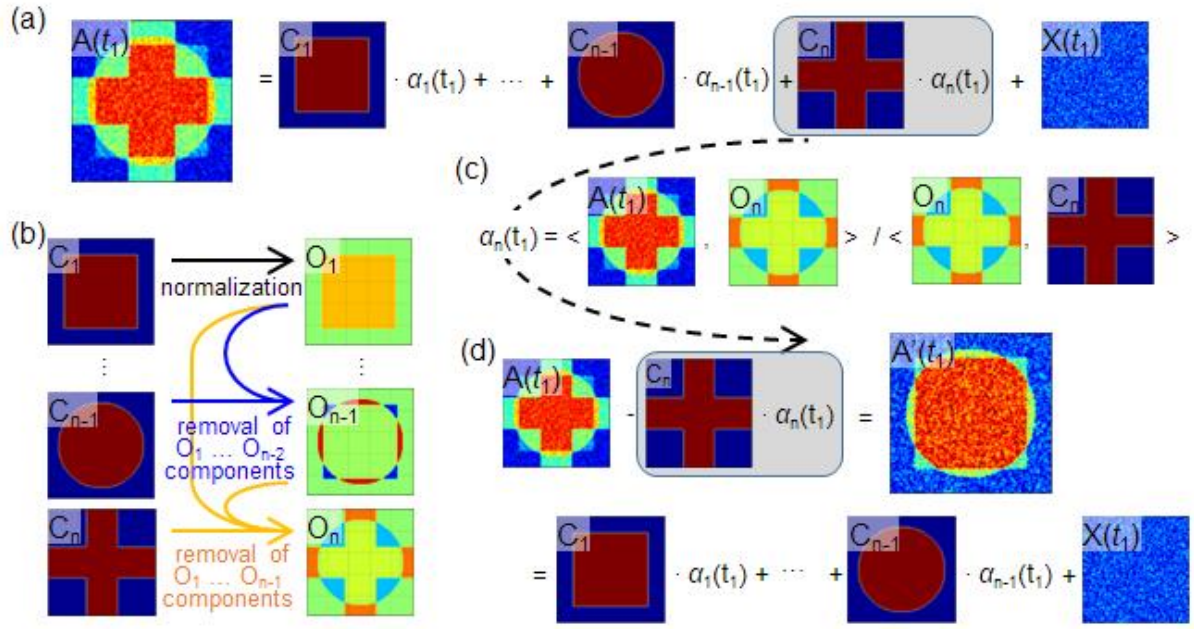

FIG. S1. Schematic diagram illustrating LCF using the direct method. In this figure, the experimental signal and its components are displayed as two-dimensional matrices instead of column vectors for better visibility. (a) Time-resolved experimental data, $A(t_1)$, measured at a certain time delay, t_1, can be expressed as a weighted sum of signal components, C_is, having different physical origins and a residual, $X(t_1)$. Here, the signal consists of n different components. The time-dependent weights of the components are denoted as $\alpha_i(t_1)$. (b) The first step is the Gram-Schmidt (GS) process of the components, C_is. The signal components, each of which has its own physical origin, C_i, are not necessarily orthogonal. Therefore, as the first step, the GS process is applied to the C_is to yield the orthonormalized components, O_is. The process proceeds step by step from C_1 to C_n. As an example, when orthonormalizing C_i, the vector components of other orthonormalized vectors from O_1 to O_{i-1} in C_i are removed to generate O_i. The resulting O_i is orthogonal to other vectors from O_1 to O_{i-1}. (c) In the second step, using the orthogonalized components obtained from (b), the weight of the C_n component, $\alpha_n(t_1)$, can be directly calculated. Here, the notation <*A*, *B*> denotes the inner product of the two vectors *A* and *B*. As also explained in Equation S8, the weight can be obtained by calculating $< A(t_1), O_n > / < O_n, C_n >$. (d) In the third step, using the weight $\alpha_n(t_1)$ calculated from (c), the contribution of C_n can be removed from $A(t_1)$ by subtracting $\alpha_n(t_1) \cdot C_n$. The resulting remnant experimental data, $A'(t_1)$, now consists of $n-1$ different components. In the fourth step, the procedures (c) and (d) are repeated until $\alpha_1(t_1)$ is obtained. Thus, the weights from $\alpha_n(t_1)$ to $\alpha_1(t_1)$ can be retrieved.

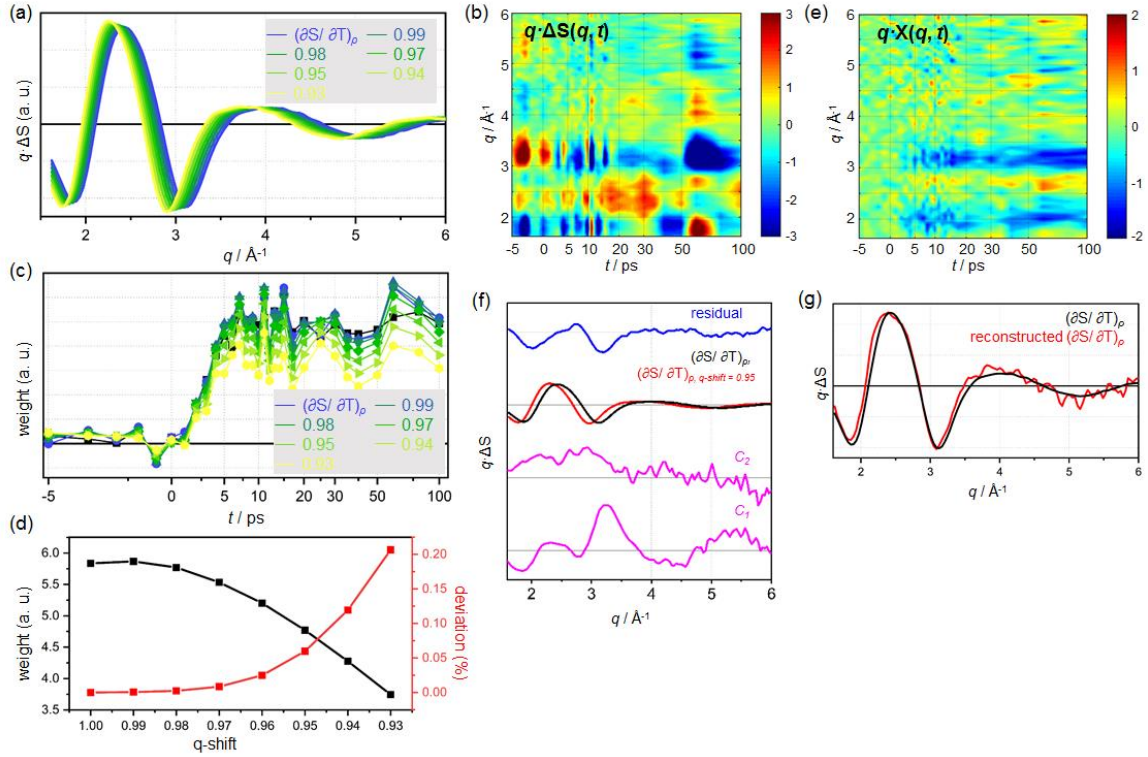

FIG. S2. The effect of errors in the prior knowledge and the reconstruction of the correct $(\partial S(q)/\partial T)_\rho$ curve even when an erroneous $(\partial S(q)/\partial T)_\rho$ curve is used as the input for SANOD. (a) Various erroneous $(\partial S(q)/\partial T)_\rho$ curves were generated by distorting the correct $(\partial S(q)/\partial T)_\rho$ along the q-axis. The values in the legend indicate the q-shift applied to generate the distorted curves. (b) Experimental data, which is the same as Figure 4a. (c) The $\alpha_3(t)$ traces obtained by SANOS using various $(\partial S(q)/\partial T)_\rho$ curves as the prior knowledge for the analysis of the data shown in Figure 4a in the main text. (d) The contributions (left y-axis) of the prior knowledge component and the deviations (right y-axis) of the $\alpha_3(t)$ traces from that obtained from the correct $(\partial S(q)/\partial T)_\rho$ or $U_1(q)$ are plotted as the function of the q-shift. (e) The residual obtained when an erroneous $(\partial S(q)/\partial T)_\rho$ curve with the q-shift of 0.95 is used. Unlike the case where $U_1(q)$ or the correct $(\partial S(q)/\partial T)_\rho$ curve is used, the residual is not negligible any more. (f) The components used for SANOD. The black curve is the correct $(\partial S(q)/\partial T)_\rho$ and the red curve is an erroneous one with the q-shift of 0.95. C_1 and C_2 are the major components from the SVD of the data at negative time delays. C_1, C_2 and the erroneous $(\partial S(q)/\partial T)_\rho$ were used as the input for SANOD. The blue curve is the major component that has the $\alpha_3(t)$ trace, extracted from the residual in (e). (g) Comparison of the correct $(\partial S(q)/\partial T)_\rho$ curve (black) and the reconstructed $(\partial S(q)/\partial T)_\rho$ curve (red) obtained by using the residual from the SANOD using the erroneous $(\partial S(q)/\partial T)_\rho$ curve. We note that the correct $(\partial S(q)/\partial T)_\rho$ can be still obtained by using either $U_1(q)$ (as described in the section C of the supplementary material) or even the inaccurate, erroneous prior knowledge on the shape of the signal component (as described in the section D of the supplementary material).

IV. Supplementary References

[1]Åke Björck, BIT Numer. Math. **7**, 1 (1967).

[2]Kenneth Hoffman and Ray Alden Kunze, *Linear algebra*, 2nd (Prentice-Hall, Upper Saddle River, New Jersey, 1971), p.280.

[3]J. W. Daniel, W. B. Gragg, L. Kaufman, and G. W. Stewart, Math. Comp. **30**, 772 (1976).

[4]Walter Hoffmann, Computing **41**, 335 (1989).

[5]E. W. Cheney and David Kincaid, *Linear Algebra: Theory and Applications* (Jones and Bartlett Publishers, Sudbury, Mass., 2009), p.544.

[6]Alston S. Householder, J. ACM **5**, 339 (1958).

[7]David D. Morrison, J. ACM **7**, 185 (1960).

[8]C. Donald La Budde, Math. Comp. **17**, 433 (1963).

[9]Peter Businger and Gene H. Golub, Numer. Math. **7**, 269 (1965).

[10]William H. Press, Saul A. Teukolsky, William T. Vetterling, and Brian P. Flannery, *Numerical recipes: the art of scientific computing*, 3rd (Cambridge University Press, New York, 2007), p.578.

[11]Åke Björck, *Numerical methods for least squares problems* (SIAM, Philadelphia, 1996), p.54.

[12]C. W. Ahn, H. Ki, J. Kim, J. Kim, S. Park, Y. Lee, K. H. Kim, Q. Y. Kong, J. Moon, M. N. Pedersen, M. Wulff, and H. Ihee, J. Phys. Chem. Lett. **9**, 647 (2018).

[13]K. H. Kim, J. G. Kim, S. Nozawa, T. Sato, K. Y. Oang, T. Kim, H. Ki, J. Jo, S. Park, C. Song, T. Sato, K. Ogawa, T. Togashi, K. Tono, M. Yabashi, T. Ishikawa, J. Kim, R. Ryoo, J. Kim, H. Ihee, and S. Adachi, Nature **518**, 385 (2015).

[14]K. H. Kim, J. G. Kim, K. Y. Oang, T. W. Kim, H. Ki, J. Jo, J. Kim, T. Sato, S. Nozawa, S. Adachi, and H. Ihee, Struct. Dyn. **3** (2016).